

Liver transplantation is acknowledged as the treatment of choice for patients with early, unresectable HCC and the Milan criteria have been widely accepted for selection of HCC patients for transplantation [18,19]. On the contrary, Kaihara *et al.* [5] reported that the 20 HCC patients beyond the Milan criteria showed tumour-free survival of approximately 50% at 2 years after LDLT. These results demonstrated the considerable possibility that even HCC patients, who had been excluded by the Milan criteria, can survive for long periods after transplantation. In our institution, all HCC patients have the extent of tumour involvement evaluated with abdominal, chest and brain CT scans, and by bone scintigraphy within the 2 months before transplantation; but condition, number and size of the tumours are not criteria for exclusion. The present patient underwent LDLT for HCC beyond the Milan criteria. However, as he would get the opportunity for long-term survival, long-term arterial graft patency would be necessary.

In conclusion, we believe that this report is the first documented use of an autologous radial artery for interpositional artery graft in LDLT for HCC patients. Although the radial artery is not a first-line arterial conduit, it can safely and successfully be used when a suitable recipient's artery is unavailable and the use of a saphenous vein or other conduits is believed to be undesirable. Autologous radial artery grafts should be added to the transplant surgeon's armamentarium as needed for interpositional artery graft in LDLT patients who have undergone repeated intraarterial chemotherapy for HCC.

References

- Garcia VJ, Grande L, Rimola A, Fuster J, Lacy A, Visa J. The use of the saphenous vein for arterial reconstruction in orthotopic liver transplantation. *Transplant Proc* 1990; 22: 2376.
- Sansalone CV, Colella G, Rondinara GF, *et al.* Iliac artery graft interposition in liver transplantation: our experience in 72 cases. *Transplant Proc* 1994; 26: 3535.
- Nakatsuka T, Takushima A, Harihara Y, Makuuchi M, Kawarasaki H, Hashizume K. Versatility of the inferior epigastric artery as an interpositional vascular graft in living-related liver transplantation. *Transplantation* 1999; 67: 1490.
- Santamaria ML, Vazquez J, Gamez M, *et al.* Donor vascular grafts for arterial reconstruction in pediatric liver transplantation. *J Pediatr Surg* 1996; 31: 600.
- Kaihara S, Kiuchi T, Ueda M, *et al.* Living-donor liver transplantation for hepatocellular carcinoma. *Transplantation* 2003; 75: 37.
- Calafiore AM, Di Giammarco G, Teodori G, *et al.* Radial artery and inferior epigastric artery in composite grafts: improved midterm angiographic results. *Ann Thorac Surg* 1995; 60: 517.
- Reyes AT, Frame R, Brodman RF. Technique for harvesting the radial artery as a coronary artery bypass graft. *Ann Thorac Surg* 1995; 59: 118.
- Kurokohchi K, Watanabe S, Masaki T, *et al.* Combined use of percutaneous ethanol injection and radiofrequency ablation for the effective treatment of hepatocellular carcinoma. *Int J Oncol* 2002; 21: 841.
- Murata K, Shiraki K, Kawakita T, *et al.* Low-dose chemotherapy of cisplatin and 5-fluorouracil or doxorubicin via implanted fusion port for unresectable hepatocellular carcinoma. *Anticancer Res* 2003; 23: 1719.
- Dabboussi M, Saade YA, Poncet A, Baehrel B. Fistula between a saphenous vein graft aneurysm and the pulmonary artery trunk. *Ann Thorac Surg* 2001; 71: 1356.
- Kusagawa H, Hiraiwa T, Hata H, Takanaka C. Surgical repair of a pseudoaneurysm derived from a nine-year-old saphenous vein graft after coronary artery bypass. *Jpn J Thorac Cardiovasc Surg* 2002; 50: 129.
- Campeau L, Enjalbert M, Lesperance J, Vaislic C, Grondin CM, Bourassa MG. Atherosclerosis and late closure of aorto-coronary saphenous vein graft: sequential angiographic studies at 2 weeks, 1 year, 5-7 years, and 10-12 years after surgery. *Circulation* 1983; 68: 1.
- Carpentier A, Guermonprez JL, Deloche A, Frechette C, DuBost C. The aorta-to-coronary radial artery bypass graft: a technique avoiding pathological changes in grafts. *Ann Thorac Surg* 1973; 16: 111.
- Acar C, Jebara VA, Portoghesi M, *et al.* Revival of the radial artery for coronary artery bypass grafting. *Ann Thorac Surg* 1992; 54: 652.
- Dietl CA, Benoit CH. Radial artery graft for coronary artery revascularization: technical considerations. *Ann Thorac Surg* 1995; 60: 102.
- Acar C, Ramsheji A, Pagny JY, *et al.* The radial artery for coronary artery bypass grafting: clinical and angiographic results at five years. *J Thorac Cardiovasc Surg* 1998; 116: 981.
- Nunoo-Mensah J. An unexpected complication after harvesting of the radial artery for coronary artery bypass grafting. *Ann Thorac Surg* 1998; 66: 929.
- Llovet JM, Bruix J, Fuster J, *et al.* Liver transplantation for small hepatocellular carcinoma: the tumor-node-metastasis classification does not have prognostic power. *Hepatology* 1998; 27: 1572.
- Bismuth H, Majno P, Adam R. Liver transplantation for hepatocellular carcinoma. *Semin Liver Dis* 1999; 19: 311.

Outflow block secondary to stenosis of the inferior vena cava following living-donor liver transplantation?

Mizuno S, Yokoi H, Yamagiwa K, Tabata M, Isaji S, Yamakado K, Takeda K, Uemoto S. Outflow block secondary to stenosis of the inferior vena cava following living-donor liver transplantation?
 Clin Transplant 2004 DOI: 10.1111/j.1399-0012.2004.00321.x
 © Blackwell Munksgaard, 2004

Shugo Mizuno^a, Hajime Yokoi^a,
 Kentaro Yamagiwa^a,
 Masami Tabata^a, Shuji Isaji^a,
 Koichiro Yamakado^b, Kan Takeda^b
 and Shinji Uemoto^a

^a First Department of Surgery and ^b Department of Radiology, Mie University School of Medicine, Mie, Japan

Abstract: Although it is well known that outflow block is caused by stenosis or occlusion of hepatic vein anastomoses following living donor liver transplantation (LDLT), there have been few reports on inferior vena cava (IVC) stenosis following LDLT. In this paper, we report two cases of IVC stenosis and hepatic vein outflow block following right hepatic LDLT in the absence of stenosis of any of the anastomoses. Both patients presented with liver dysfunction, an ascitic fluid volume of approximately 2000 mL, and congestion in their biopsy specimens, and venocavography demonstrated IVC stenosis with gradients of more than 10 mmHg in patients with a dominant inferior right hepatic vein (IRHV) anastomosis. After a Gianturco expandable metallic stent successfully implanted in the IVC, the patient's liver function recovered and the volume of ascitic fluid decreased. The pathogenesis of hepatic vein outflow block secondary to IVC stenosis following LDLT may involve the anastomosis with the IRHV, which is the dominant draining vein of the graft and larger than the RHV, caudal to the IVC stenosis and a significant IVC pressure gradient that results in increased IRHV pressure. In conclusion, it is important to include hepatic vein outflow block in the differential diagnosis when patients who have undergone right hepatic LDLT in which anastomosis of the large IRHV has been performed develop manifestations of liver dysfunction.

Key words: Gianturco Z stent – inferior vena cava stenosis – living-donor liver transplantation – outflow block

Corresponding author: Shugo Mizuno, First Department of Surgery, Mie University School of Medicine, 2-174 Edobashi, Tsu, Mie, 514-0001, Japan.
 Tel.: +81 59 232 1111 (ext. 6470);
 fax: +81 59 232 8095;
 e-mail: mizuno-s@clin.medic.mie-u.ac.jp

Accepted for publication 27 October 2004

Outflow block or Budd-Chiari syndrome after orthotopic liver transplantation (OLT) develops as a result of anastomotic stenosis or occlusion of the inferior vena cava (IVC), whereas almost all cases of outflow block syndrome after living donor liver transplantation (LDLT) are the result of stenosis or occlusion of the hepatic vein anastomosis. These potentially lethal complications are manifested by deteriorating hepatic and renal function, hypotension, declining cardiac output, edema of the lower extremities, and massive ascites (1, 2). However, there have been few reports of outflow block syndrome in patients who developed IVC stenosis with a pressure gradient greater than 10 mmHg after LDLT in the absence of stenosis or occlusion of the hepatic vein anastomosis. We

report two cases of IVC stenosis and outflow block syndrome that developed following right hepatic LDLT with dominant inferior right hepatic vein (IRHV) anastomosis in which the outflow block syndrome was treated by insertion of a Gianturco expandable metallic stent.

Patients and methods

Between March 2002 and July 2004 we performed 44 adult-to-adult LDLT procedures (including two re-transplantations) at our hospital. The 39 patients (27 men, 12 women; 41 operations) who received a right liver graft were the subjects of the

present study. The patient's ages ranged from 20 to 68 yr old (median age = 53 yr). The indications for LDLT were hepatocellular carcinoma (n = 17), hepatitis C viral cirrhosis (n = 10), primary biliary cirrhosis (n = 4), hepatitis B viral cirrhosis (n = 2), cryptogenic cirrhosis (n = 2), fulminant hepatic failure (n = 2), chronic rejection (n = 2), primary sclerosing cholangitis (n = 1), and biliary atresia (n = 1).

Donors

The donors were 20 men and 21 women, and their ages ranged from 18 to 63 yr old (median age = 36 yr). According to their relation to the patient they consisted of 17 children, 15 spouses, five sibling, two parents, one nephew, and one grandchild. Right liver volume was preoperatively estimated by computed tomography (CT). Candidates whose right liver comprised more than 70% of their whole liver were rejected as prospective donors. An estimated graft-to-recipient weight ratio (GRWR) of 0.8 was the lower limit for right liver transplantation. Right liver grafts without the middle hepatic vein (MHV) were harvested; however, when the remnant left liver was estimated to account for more than 35% of the whole liver volume, harvesting an extended right liver graft was considered. We reconstructed all MHV tributaries that measured more than 5 mm in diameter with interpositional vascular grafts such as the recipient's inferior mesenteric vein, left portal vein, umbilical vein, or other veins.

Hepatic vein reconstructions procedure

The anastomoses between the graft vein and IVC were created in end-to-side fashion with 5-0 or 6-0 prolene stitches as described previously (3). The RHV anastomoses were performed by incising the IVC at the caudal corner of the RHV orifice and removing a piece of the anterior IVC wall to make the orifice oval-shaped. For the other anastomoses, a new hole was made by removing a small part of the IVC wall.

Results

Morbidity and mortality related to venous reconstruction

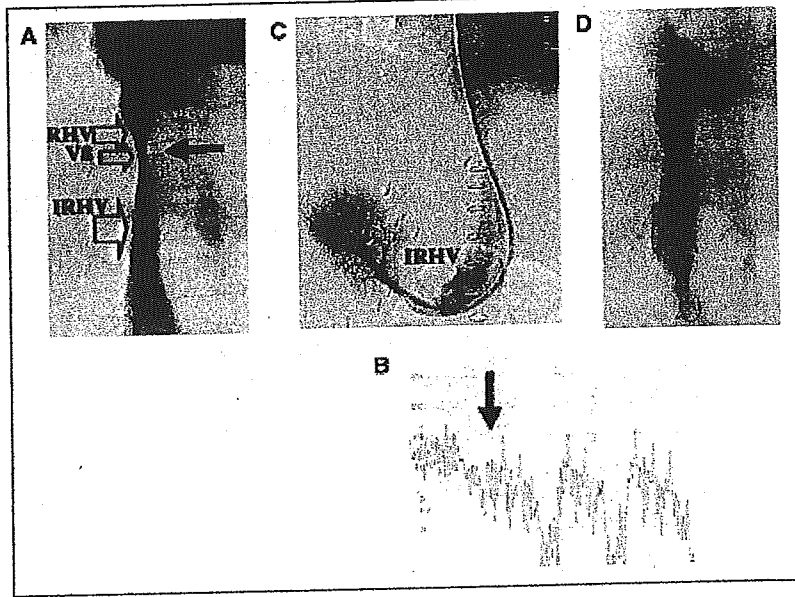
No patients died of complications of the venous reconstructions after LDLT. Four patients (9.7%) experienced complications of the venous reconstructions in the form of outflow block syndrome, and all were successfully treated with metallic

stents. Stenosis of the hepatic vein anastomosis developed as a complication in one of these patients, and a rare complication, totuous intrahepatic stenosis of the hepatic venous trunk, occurred in another patient (4). The remaining two cases of outflow block syndrome were suspected of being secondary to stenosis of the IVC with a pressure gradient greater than 10 mmHg, and they were described below.

Case 1

The patient was a 51-yr-old man with a history of liver dysfunction secondary to hepatitis C since 1990. LDLT of the right hepatic lobe of the patient's cousin was performed in July 2003, and the RHV and IRHV of the graft were anastomosed to the IVC of the recipient. The recipient's umbilical vein was used as an interpositional vascular graft between the major hepatic vein from segment VIII (V8) and the IVC. The diameter of the RHV, IRHV, and V8 was 15, 35, and 11 mm respectively. The GRWR was 1.15. Intraoperative Doppler ultrasound examinations did not reveal any evidence of stenosis or obstruction of hepatic venous, portal venous, or hepatic arterial blood flow. The patient's aspartate transaminase (AST), alanine aminotransferase (ALT), and total bilirubin (T-bil) levels had increased to 179, 215 IU/mL, and 14.9 mg/dL, respectively, on postoperative day (POD) 10, and daily measurements of ascitic fluid volume from a percutaneous drainage tube showed an increase to more than 1000 mL from POD 6 onwards. Doppler ultrasound examinations on POD 10 revealed flat waveforms and slightly low flow velocities in the RHV, IRHV, and V8 of 30, 18, and 9 cm/s, respectively, and a slightly low flow velocity of 15 cm/s in the right main portal vein. There were no areas of congestion on a CT scan. Hepatic venography and venacavography were performed on POD 10 because of clinical suspicion that hepatic venous obstruction had developed. The hepatic venograph showed no evidence of stenosis and no pressure gradients across any of the hepatic vein anastomoses. However, IVC stenosis was visualized by venacavography, and manometric venous pressure data from the infrahepatic IVC to the suprahepatic IVC obtained by drawing a catheter through the vessel revealed a pressure gradient of 11 mmHg across the IVC stenosis (Fig. 1A,B). The large IRHV anastomosis with no stenosis was located caudal to the site of stenosis (Fig. 1C). A 30 mm diameter, 5 cm long Gianturco Z stent (Cook, Bloomington, IN, USA) was placed in the

Fig. 1. (A) Venacavography in case 1, showing IVC stenosis associated with an 11 mmHg gradient (black arrow). The locations of the right hepatic vein (RHV), major hepatic vein from segment VIII (V8), and inferior right hepatic vein (IRHV) anastomoses are demonstrated. (B) Manometric venous pressure data showing a pressure gradient of 11 mmHg across the IVC stenosis (the black arrow indicates the same site as in A). (C) Hepatic venography of the IRHV revealing no evidence of stenosis or narrowing of the anastomosis. (D) After deployment of the IVC stent, there is ample IVC patency and only a 1 mmHg residual pressure gradient.



IVC, and the venous pressure gradient immediately decreased to 1 mmHg (Fig. 1D). The reason for choosing this stent is that the Z stent has wide interstices that minimize interference with hepatic vein outflow. Liver function also gradually improved after stent placement, and the daily ascitic fluid volume decreased to < 500 mL from POD 16 onwards (Fig. 2). Stent placement was successful, and the patency of the stent remains good. The patient was discharged on POD 43, and his course has been favorable over the 14 months since the operation.

Case 2

The patient was a 54-yr-old man with liver failure secondary to hepatitis C and was referred to our department for LDLT in April 2003. LDLT of the right hepatic lobe of the patient's son was performed, and the RHV of the graft was anastomosed to the IVC of the recipient in end-to-side fashion. The IRHV and the major hepatic veins from segment V (V5) and V8 were anastomosed to the side of the recipient's IVC. The recipient's left portal vein was used as an interpositional vascular

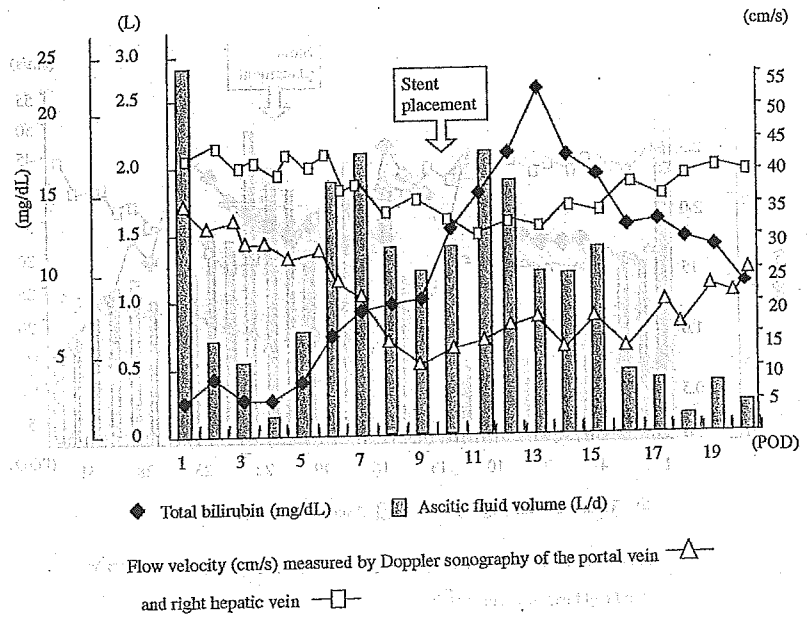


Fig. 2. Clinical course in case 1 before and after stenting. The closed squares represent serum total bilirubin (mg/dL). The shaped bars represent daily ascitic fluid (L). The open triangles and open squares represent flow velocity (cm/s) measured by Doppler ultrasound in the portal vein and the right hepatic vein respectively.

graft for the V5 anastomosis, and the recipient's inferior mesenteric vein was used as an interpositional graft for the V8 anastomosis. The diameter of the RHV, IRHV, V5, and V8 was 25, 10, 11, and 28 mm respectively. The GRWR was 1.12. Intraoperative Doppler ultrasound examinations did not reveal any evidence of stenosis or obstructions in the hepatic venous, portal venous, or hepatic arterial blood flow. The patient's AST, ALT, and T-bil levels had increased to 228, 196 IU/mL, and 36.5 mg/dL, respectively, on POD 15. Daily ascitic fluid volume from the percutaneous drainage tube increased from below 1000 mL to more than 2000 mL from POD 14 onwards. Ascitic fluid cultures were negative. Doppler ultrasound examinations revealed flat waveforms, flow velocity in the RHV, IRHV, V8, and V5 of 31, 28, 11, and 13 cm/s, respectively, and a flow velocity of 21 cm/s in the right main portal vein. No areas of congestion were visible on a CT scan. Steroid pulse therapy was started, because of strong suspicion of acute rejection, but there was no improvement in the liver dysfunction. A liver biopsy demonstrated centrilobular congestion, and hepatic venography was performed on POD 20 because of clinical suspicion that hepatic venous obstruction had developed. The hepatic venograph showed no evidence of stenosis and no pressure gradients across any of the hepatic vein anastomoses. However, IVC stenosis was visualized by venacavography, and manometric venous pressure data from the infrahepatic IVC to the suprahepatic IVC obtained by drawing a catheter through the vessel revealed a pressure gradient of 13 mmHg across

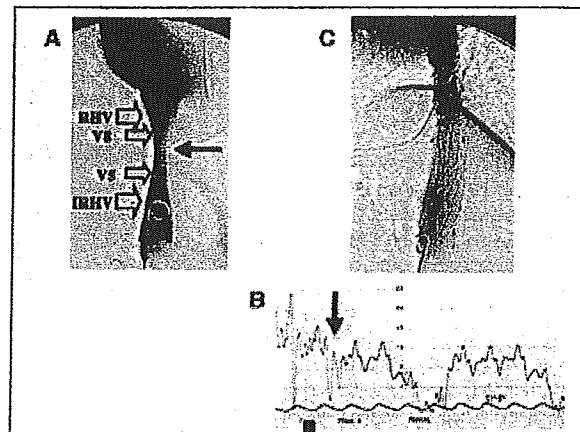


Fig. 3. (A) Venacavography in case 2, showing IVC stenosis associated with 13 mmHg gradient (black arrow). The locations of the anastomoses with RHV, V5, V8 and, IRHV are demonstrated. (B) Manometric venous pressure data showing a pressure gradient of 13 mmHg across the IVC stenosis (the black arrow indicates the same site as in A). (C) After deployment of the IVC stent, there is ample IVC patency and a residual 3 mmHg pressure gradient.

the IVC stenosis (Fig. 3A,B). A 35-mm diameter, 5-cm long Gianturco Z stent was placed in the IVC. The venous pressure gradient immediately decreased to 3 mmHg (Fig. 3C), and liver function gradually improved. The AST, ALT, and T-bil levels had decreased to 45, 64 IU/L, and 9.6 mg/dL, respectively, on POD 40. Daily ascitic fluid volume decreased to <1000 mL from POD 40 onwards, and continued to decrease to <500 mL from POD 46 onwards (Fig. 4). Unfortunately the

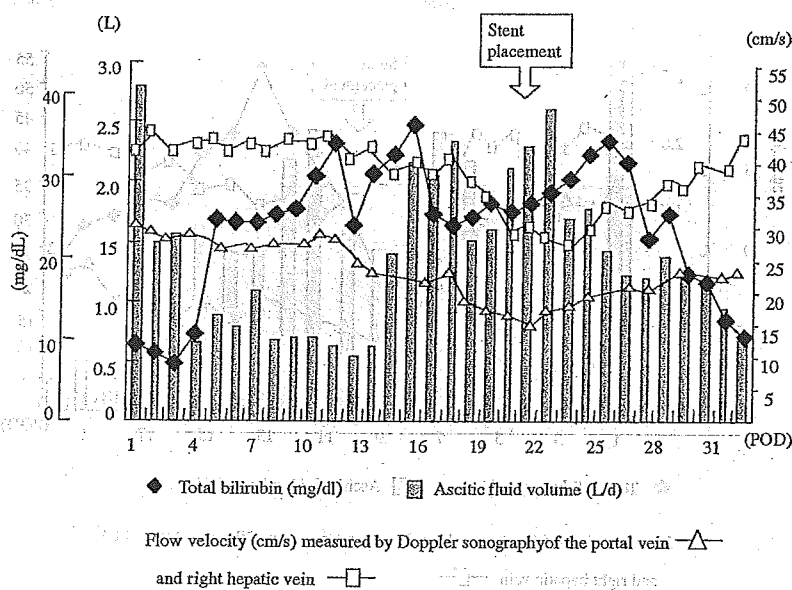


Fig. 4. Clinical course in case 2 before and after stenting. The closed squares represent serum total bilirubin (mg/dL). The shaped bars represent daily ascitic fluid volume (L). The open triangles and open squares mean represent flow velocity (cm/s) measured by Doppler ultrasound of the portal vein and the right hepatic vein respectively.

patient died on POD 77 as a result of massive gastrointestinal bleeding from a duodenal ulcer.

Discussion

Caval abnormalities that occur after OLT include stenosis as a result of a tight suture line or caval size mismatch, kinking or buckling of the redundant hepatic vein, external compression by a hypertrophied liver graft, torsion either due to a transplant size mismatch or transplant rotation, and fibrosis or intimal hyperplasia in the perianastomotic area (5, 6). However, Lee *et al.* reported that prolonged massive ascites of more than 10 000 mL following right hepatic LDLT could be treated with IVC metallic stents (7). It has been reported that the lateral sector of the right hepatic graft compresses the vena cava and interferes with outflow drainage through the IRHV, because congestive infarction of the right median sector, from which the major hepatic vein from V5 and V8 was not reconstructed, has been found to induce compensatory hypertrophy of the lateral sector (7). Although the major hepatic vein from V5 and V8 was reconstructed in both cases reported above and was not obstructed perioperatively, venacavography revealed IVC stenosis and a pressure gradient of more than 10 mmHg. The pathogenesis of IVC stenosis may be a narrowing of the IVC caused by the multiple anastomoses of major hepatic tributaries to the cut surface of the graft and compression caused by hypertrophy of the grafted liver.

Not all patients with IVC stenosis with a pressure gradient develop hepatic vein outflow block. The pathogenesis of hepatic vein outflow block secondary to IVC stenosis following right hepatic LDLT may involve the anastomosis of the IRHV, which is the dominant draining vein of the graft and larger than the RHV, caudal to the IVC stenosis and a significant IVC pressure gradient that results in increased IRHV pressure. Hepatic

vein outflow block does not occur in cases of IVC stenosis with significant pressure gradients that develop after left hepatic LDLT or right hepatic LDLT without dominant IRHV anastomosis, because the left hepatic vein and RHV anastomoses are located cranial to the stenosis, and thus the stenosis is unaffected by left hepatic or RHV vein pressure.

In conclusion, in both cases reported above IVC stenosis and hepatic vein outflow block developed following right hepatic LDLT with dominant IRHV anastomosis and were treated with a Gianturco Z stent implant. It is important to include hepatic vein outflow block in the differential diagnosis when patients who have undergone right hepatic LDLT in which anastomosis of the large IRHV has been performed develop manifestations of liver dysfunction.

References

1. LERUT J, TZAKIS AG, BROUN K et al. Complications of venous reconstruction in human orthotopic liver transplantation. *Ann Surg* 1987; 205: 404.
2. ORONS PD, ZAJKO AB. Angiography and interventional procedures in liver transplantation. *Radiol Clin North Am* 1995; 33: 541.
3. TANAKA K, INOMATA Y, KAIHARA S. Living-Donor Liver Transplantation. Surgical Techniques and Innovations. Surgical Procedure for Hepatic Vein Reconstruction. Barcelona, Spain: Prous Science, 2003.
4. YAMAGIWA K, YOKOI H, ISAJI S et al. Intrahepatic hepatic vein stenosis after living-related liver transplantation treated by insertion of an expandable metallic stent. *Am J Transplant* 2004; 4: 1006.
5. ZAJKO AB, CLAUS D, CLAPUYT P et al. Obstruction to hepatic venous drainage after liver transplantation: treatment with balloon angioplasty. *Radiology* 1989; 170: 763.
6. SIMO G, ECHENAGUSIA A, CAMUNEZ F et al. Stenosis of the inferior vena cava after liver transplantation: treatment with Gianturco expandable metallic stents. *Cardiovasc Intervent Radiol* 1995; 18: 212.
7. LEE SG, PARK KM, HWANG S et al. Congestion of right liver graft in living donor liver transplantation. *Transplantation* 2001; 71: 812.

Intrahepatic Hepatic Vein Stenosis After Living-Related Liver Transplantation Treated by Insertion of an Expandable Metallic Stent

Kentaro Yamagiwa^{a,*}, Hajime Yokoi^a,
Shuji Isaji^a, Masami Tabata^a, Shugo Mizuno^a,
Tomohide Hori^a, Koichiro Yamakado^b,
Shinji Uemoto^a and Kan Takeda^b

^aFirst Department of Surgery, and

^bDepartment of Radiology, Mie University School of
Medicine, Tsu City, Mie Prefecture, Japan

*Corresponding author: Kentaro Yamagiwa,
yamagw-k@clin.medic.mie-u.ac.jp

Although the incidence of stenosis and obstruction of the hepatic venous anastomosis after right hepatic living-related liver transplantation (LRLT) has been found to be higher than after orthotopic liver transplantation (OLT), to the best of our knowledge, intrahepatic stenosis of the venous trunk in the early period after right hepatic LRLT has never been reported in the literature. A 53-year-old man who underwent right hepatic LRLT; postoperatively, developed liver dysfunction and an increasing amount of ascites, and a Doppler sonogram showed a flat waveform and low-flow velocity in the hepatic vein. Based on these findings an outflow block was suspected, and a hepatic venogram and manometry revealed intrahepatic stenosis of a tortuous hepatic venous trunk and a pressure gradient of 14 mmHg at the site of the stenosis. We inserted an expandable metallic stent (EMS) at the site of intrahepatic venous stenosis, and its insertion was followed by a decrease in pressure gradient. Liver function recovered, and the volume of ascitic fluid decreased after placement of the EMS. The results of an analysis of the venogram and CT volumetric data suggested that the pathogenesis of the stenosis was twisting of the venous trunk during hypertrophy of the liver parenchyma.

Key words: EMS, hepatic vein stenosis, liver regeneration, LRLT

Received 4 October 2003, revised and accepted for publication 4 February 2004

Introduction

Right hepatic living-related liver transplantation (LRLT) is now commonly used to treat adults, and although steno-

sis of the right hepatic vein anastomosis has been found to occur as a postoperative complication, to our knowledge early intrahepatic hepatic venous stenosis not at the site of the anastomosis has never been reported. We report such a case and describe the radiological findings obtained by hepatic venography and the hepatic vein manometric data in a patient treated with an expandable metallic stent (EMS). We discuss the possible pathogenetic mechanism of the intrahepatic stenosis of the hepatic vein that developed during the period of liver regeneration after right hepatic LRLT.

Case Report

A 53-year-old man was referred to our department for LRLT. At 39 years of age he had been diagnosed with liver dysfunction secondary to hepatitis B virus (HBV) infection. Liver cirrhosis and hepatocellular carcinoma (HCC) subsequently developed, and he was treated by trans-arterial embolization at 48 years of age. The HCC recurred at 52 years of age, and he developed an umbilical hernia caused by a huge volume of ascitic fluid. Living-related liver transplantation of an ABO-compatible right hepatic lobe donated by his wife was performed. Preoperative three-dimensional dynamic enhanced computed tomography of the donor revealed that drainage veins from the middle hepatic vein had not developed in Couinaud segments V and VIII, that the main drainage route of venous return from right lobe of the liver was the right hepatic vein, and that there was no stenosis (Figure 1). The graft-to-recipient weight ratio was 0.89%. The main hepatic vein of the donor was anastomosed to the right hepatic vein of the recipient without reconstruction of the middle hepatic vein. The length of the orifice and the cuff of the right hepatic vein of the graft were 27 mm and 14 mm, respectively, and the length of the remnant right hepatic vein of the recipient was 8 mm. The detailed surgical procedure for hepatic vein reconstruction was as follows. The vascular clamp holding the stump of the right hepatic vein was positioned vertically on the inferior vena cava (IVC). The IVC was incised at the inferior end of the right hepatic vein orifice to adjust it to the length of the orifice of the hepatic vein of the graft. A portion of the anterior wall of the IVC was removed to make the orifice oval-shaped. End stitches of 5–0 polypropylene monofilament suture were placed on the superior and inferior ends. The superior stitch of

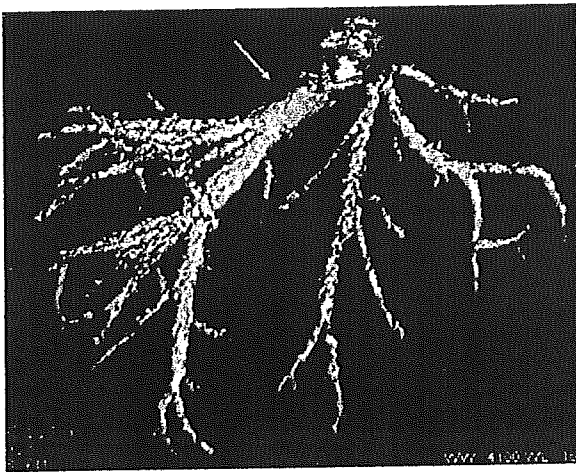


Figure 1: Three-dimensional dynamic-enhanced computed tomography of the donor's liver showing that the main drainage route of venous return of the right lobe was the right hepatic vein (white arrow), and absence of stenosis.

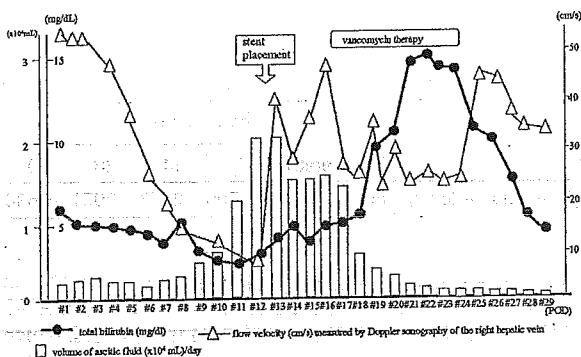


Figure 2: Sequential changes in the serum total bilirubin level (●), volume of ascitic fluid (□), and flow velocity (Δ) measured by Doppler sonography of the right hepatic vein after the operation. Flow velocity increased greatly after placement of an expandable metallic stent, and the volume of ascitic fluid decreased. The serum total bilirubin level increased to 15 mg/dL because of sepsis, but decreased in response to Vancomycin therapy.

...obstructed to caused noncappo... (text is partially obscured and difficult to read due to image quality and scanning artifacts).

a catheter inserted into the superior mesenteric vein via a branch of the ileocolic vein. Before hepatectomy, it was 33 mmHg, but it decreased to 20 mmHg after transplantation, and ultimately to 9 mmHg on postoperative day (POD) 7. HbIg and lamivudine were given postoperatively, and immunosuppressive treatment with tacrolimus was started immediately after transplantation. On POD 10 the serum aspartate aminotransferase (AST), alanine aminotransferase (ALT), and total bilirubin (T-bil) values had decreased to 56 international units (IU)/mL, 41 IU/mL, and 2.8 mg/dL, respectively (Figure 2), and by POD 12 they had increased to 103 IU/mL, 81 IU/mL, and 3.6 mg/dL, respectively. The daily volume of ascitic fluid increased from less than 5000 mL to more than 10 000 mL on POD 11 (Figure 2). Ascitic fluid cultures were negative for mycobacteria and fungi, and no cytomegalovirus-antigen was detected on granulocytes in the ascitic fluid. A Doppler ultrasound examination on POD 12 revealed flat waveforms and low-flow velocity of 9.6 cm/s in the right hepatic vein (Figure 2), and a low-flow velocity of 11.7 cm/s in the right main portal vein. A hepatic venogram was performed on POD 13 because of clinical suspicion that hepatic venous obstruction had developed. The venogram showed stenosis of an intrahepatic vein, not of the anastomosis (Figure 3A), and examination of both the anterior-posterior view and lateral view (Figure 3B) hepatic venograms revealed that the stenotic intrahepatic vein was tortuous. Manometric venous pressure data obtained by withdrawing the catheter from the intrahepatic vein into the inferior vena cava showed a gradient of 14 mmHg across the intrahepatic stenosis (Figure 3C). The wedge pressure of the distal hepatic vein branch was 33 mmHg. We immediately inserted an EMS (diameter: 1.4 cm, length: 5 cm; Wallsten™, Boston Scientific, Nagoya, Japan K. K) into the right hepatic vein via the right internal jugular vein (Figure 4A), and the venous pressure gradient was found to have decreased to 4 mmHg (Figure 4B). A Doppler ultrasound examination after EMS placement showed a pulsatile waveform in the right hepatic vein and an increase in flow velocity at the same sites in the intrahepatic vein and the right main portal vein of 30.9 cm/s and 23.9 cm/s, respectively. The AST and ALT values had decreased to 31 IU/L and 30 IU/L, respectively, on POD 14. The daily volume of ascitic fluid decreased to less than 5000 mL from POD 18 onward, and continued decreasing to less than 500 mL from POD 25 onward. The patient developed to severe sepsis caused by coagulase-negative *Staphylococcus aureus* associated with increasing AST- and T-bil-values and decreasing flow velocity from POD 16 to POD 24, but treatment with Vancomycin was followed by recovery of their values. The patient was discharged on POD 55, and he has been working and enjoying a good quality of life for the past 7 months.

Discussion

The use of right hepatic lobe grafts is a major development in LRLT and has significantly increased the graft

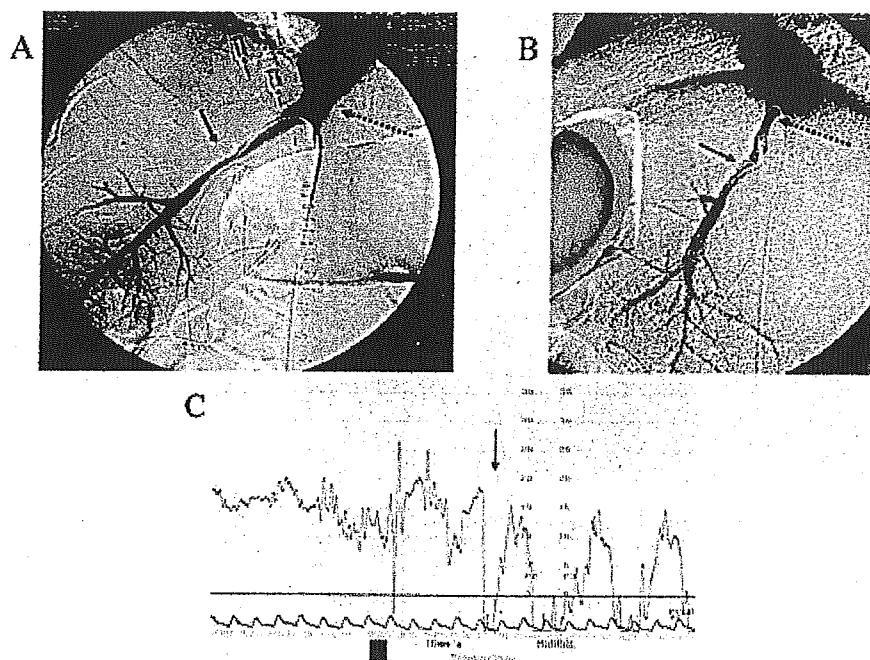


Figure 3: (A) Hepatic venogram (anterior-posterior view) and (B) hepatic venogram (lateral view). A tortuous stenotic intrahepatic vein (→) is seen, and the hepatic venous anastomosis is intact (dotted arrow). (C) Manometric hepatic venous pressure data. The hepatic venous pressure gradient was measured at the point indicated by the arrow.

supply. Right hepatic LRLT is a relatively new and technically challenging method. The hepatic venous anastomosis in a right-lobe graft is unique in terms of the variety of patterns of venous drainage, i.e. in some cases, such as our own, the right hepatic vein alone drains the entire graft, whereas in other cases the major anterior segment (Couinaud segments V and/or VIII) veins drain into a middle hepatic vein, or inferior hepatic veins may provide the main venous drainage of the posterior segment. While hepatic venous complications of orthotopic liver transplantations are rare, the anatomical variations may lead to hepatic venous congestion in the absence of reconstruction of drainage branches in LRLT, or to outflow obstruction owing to an insufficient anastomotic orifice. Egawa et al. reported two cases of early onset (1 week postoperatively) and six cases of late onset (2 months or more postoperatively) hepatic vein occlusion among 152 LRLTs (45 left lobe grafts, 106 lateral segment grafts, and one right lobe graft) (1). Inomata et al. reported outflow block in one case with multiple, separate hepatic vein anastomoses among 26 right hepatic LRLTs, and they suspected that a shift in the position of the graft may have led to the obstruction of the multiple hepatic venous anastomoses (2). Other surgeons and radiologists have reported incidences of outflow block after right hepatic LRLT of 0% [0/20 (3), 0/30 (4), 0/46 (5)] and 4% (1/256). Ko et al. treated 27 cases of hepatic venous outflow obstruction after LRLT by balloon angioplasty and insertion of an EMS, and analyzed the etiologies of the obstruction (7). They concluded that the causes were fibrosis or intimal hyperplasia in the perianastomotic area, kinking or buckling of a redundant hepatic vein, external compression by a hypertrophied liver graft, a tight suture

Table 1: CT volumetric data of the recipient

	Preoperative	Postoperative day			
		7	14	28	70
Graft volume (cm ³)	860	1700	2157	2051	1636

line, and iatrogenic obstruction after stent placement in the IVC (7). In our patient, the site of stenosis was in an intrahepatic vein far from the site of the anastomosis, which provided a sufficient orifice according to the venogram. The CT volumetric data of the right hepatic lobe graft showed that graft volume had increased approximately twofold on POD 7, and approximately 2.5-fold on POD 14 (Table 1). The increase in liver volume until POD 14 may have been secondary to venous congestion of the graft. The daily volume of ascitic fluid after the operation was ranged from approximately 1000–3000 mL until POD11, however, those volumes did not indicate liver congestion because of hepatic vein stenosis caused by a technical error in the anastomosis, because daily ascitic fluid volumes of greater than 1000 mL until POD 14 have sometimes been observed in cirrhotic patients after LRLTs. As the hepatic venous obstruction appeared to have occurred around POD 13 based on the Doppler ultrasound findings, we concluded that the doubling of the preoperative graft volume on POD 7 was attributable to regeneration of liver parenchyma rather than congestion of hepatic venous return. We suspect that relatively rapid hypertrophy of the right lobe graft that was asymmetric may have led to intrahepatic twisting of the hepatic vein like a hollow tube, and resulted in outflow block. The CT volumetric data on POD 70 showed that the

Chronic inhibition of nitric oxide increases the collateral vascular responsiveness to vasopressin in portal hypertensive rats. *J Hepatol* 2004;40:234–238.

- [2] Munoz J, Albillos A, Perez-Paramo M, Rossi I, Alvarez-Mon M. Factors mediating the hemodynamic effects of tumor necrosis factor- α in portal hypertensive rats. *Am J Physiol* 1999;276:G687–G693.
- [3] Ohta M, Tarnawski AS, Itani R, Pai R, Tomikawa M, Sugimachi K, et al. Tumor necrosis factor α regulates nitric oxide synthase expression in portal hypertensive gastric mucosa of rats. *Hepatology* 1998;27:906–913.
- [4] Bucher M, Hobbhahn J, Taeger K, Kurtz A. Cytokine-mediated downregulation of vasopressin V(1A) receptors during acute endo-

toxemia in rats. *Am J Physiol Regul Integr Comp Physiol* 2002;282:R979–R984.

- [5] Kusano E, Tian S, Umino T, Tetsuka T, Ando Y, Asano Y. Arginine vasopressin inhibits interleukin-1 beta-stimulated nitric oxide and cyclic guanosine monophosphate production via the V1 receptor in cultured rat vascular smooth muscle cells. *J Hypertens* 1997;15:627–632.
- [6] Barthelmebs M, Krieger JP, Grima M, Nisato D, Imbs JL. Vascular effects of [Arg8]vasopressin in the isolated perfused rat kidney. *Eur J Pharmacol* 1996;314:325–332.

doi:10.1016/j.jhep.2004.02.032

Serum vascular endothelial growth factor-receptor 1 during liver regeneration

To the Editor:

We read with great interest the article ‘Gene expression profile in the regenerating rat liver after partial hepatectomy’ by Fukuhara et al. [1] in which their microarray data demonstrate the molecular events in regenerating rat liver. In this analysis, however, profiling of several potent angiogenic factors genes was not well documented. Recent studies suggest that angiogenic factors play an important role in inducing liver regeneration and molecular expression patterns for angiogenic factors has been studied in rat models [2–4].

Molecules important to angiogenesis include vascular endothelial growth factor (VEGF), vascular endothelial growth factor-receptor1 (VEGF-R1) and angiogenin (ANG). Selective activation of VEGF-R1 stimulates hepatocyte, but not endothelial, proliferation and reduces liver damage in mice exposed to a hepatotoxin [5]. Additionally, VEGF and ANG may be important stimulators of sinusoidal endothelial cell (SEC) proliferation during liver regeneration in vivo [5]. This is supported by observations in rodent models that serum VEGF levels peak at 72 h and ANG levels peak at 96 h after partial hepatectomy [2,6]. However, there is little data available regarding levels of angiogenic factors after partial hepatectomy in humans.

Therefore, we investigated serum levels of VEGF, VEGF-R1 and ANG in five donors of living liver transplantation during the first 7 days after partial hepatectomy (Fig. 1). All angiogenic factors were measured by ELISA (R&D Systems). Serum VEGF-R1 levels increased immediately, peaking at 2-fold baseline levels by 6 h after surgery and decreasing gradually. In contrast, VEGF levels rose slowly until the fifth post-operative day, and increased rapidly thereafter with a three-fold increase after the fifth post-operative day. ANG levels actually decreased below baseline levels just after surgery and increased after the third post-operative day. Thus, the expression patterns of VEGF, VEGF-R1 and ANG during liver regeneration of transplantation donors

were tightly regulated in sequence. Our findings suggest that VEGF-R1 expression is up-regulated just after liver resection, whereas VEGF and ANG expression is delayed

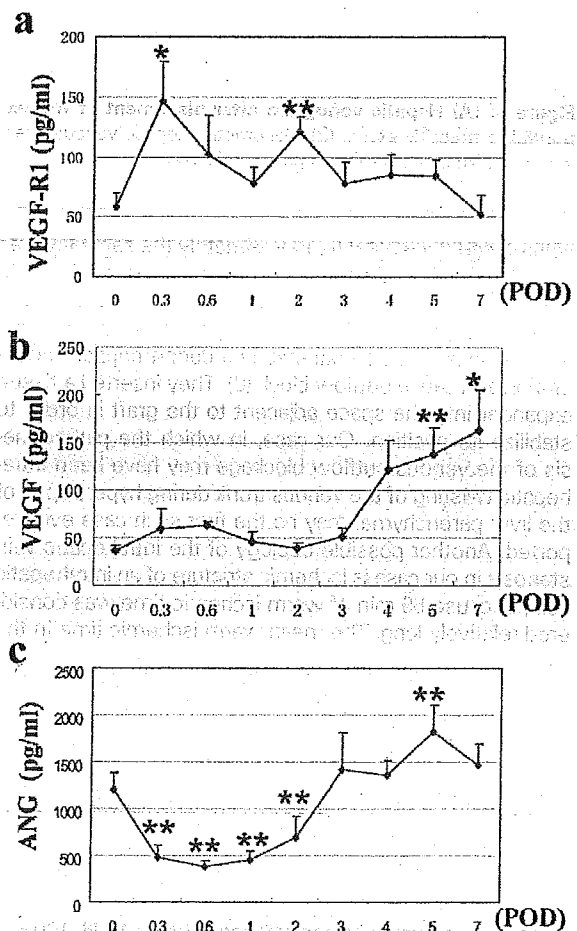


Fig. 1. (a) Serum VEGF-R1 levels (b) VEGF levels and (c) ANG levels before and after partial hepatectomy in donors. Bars indicate standard error (** $P < 0.05$ vs. 0 h, * $P < 0.1$ vs. 0 h).

by several days. Thus, in humans, VEGF-R1 may be one of the many genes up-regulated during rapid proliferation of hepatocytes after partial hepatectomy and may contribute to expression of angiogenic factors, consistent with prior studies [5]. Further evaluation of expression profiling of angiogenic factors will provide needed information about mechanisms important for liver regeneration, and future VEGF-R1 agonists may have therapeutic potential for liver regeneration.

Yukiko Saitou¹, Katsuya Shiraki¹, Yumi Yamaguchi¹,
Takeshi Nakano¹, Shugo Mizuno², Shinji Uemoto²
¹First Department of Internal Medicine,
Mie University School of Medicine, 2-174 Edobashi, Tsu,
Mie 514-8507 Japan
²First Department of Surgery,
Mie University School of Medicine, Tsu,
Mie 514-8507, Japan
E-mail address: katsuyas@clin.medic.mie-u.ac.jp

References

- [1] Fukuhara Y, Hirasawa A, Li XK, Kawasaki M, Fujino M, Fumeshima N, et al. Gene expression profile in the regenerating rat liver after partial hepatectomy. *J Hepatol* 2003;38:784–792.
- [2] Shimizu H, Miyazaki M, Wakabayashi Y, Mitsuhashi N, Kato A, Ito H, et al. Vascular endothelial growth factor secreted by replicating hepatocytes induces sinusoidal endothelial cell proliferation during regeneration after partial hepatectomy in rats. *J Hepatol* 2001;34:683–689.
- [3] Sato T, El-Assal ON, Ono T, Yamanoi A, Dhar DK, Nagasue N. Sinusoidal endothelial cell proliferation and expression of angiopoietin/Tie family in regenerating rat liver. *J Hepatol* 2001;34:690–698.
- [4] Reynaert H, Chavez M, Geerts A. Vascular endothelial growth factor and liver regeneration. *J Hepatol* 2001;34:759–761.
- [5] LeCouter J, Moritz DR, Li B, Phillips GL, Liang XH, Gerber HP, et al. Angiogenesis-independent endothelial protection of liver: role of VEGFR-1. *Science* 2003;299:890–893.
- [6] Kraizer Y, Mawasi N, Seagal J, Paizi M, Assy N, Spira G. Vascular endothelial growth factor and angiopoietin in liver regeneration. *Biochem Biophys Res Commun*. 2001;87:209–215.

doi:10.1016/j.jhep.2004.02.033

Unsatisfactory quality of hepatological information on the internet

To the Editor:

Over the last decade, a continuously growing number of web sites have been dedicated to different aspects of liver disease. Physicians, patients and health operators can now easily access to a large volume of health information resources, available on the Internet. This, however, has some pitfalls, including the potential harm associated with inaccurate or misleading information, and the possibility of commercial interests influencing the contents of medical web sites. For this reason, many organisations and academic or scientific Societies have published guidelines and rating criteria for web sites evaluation [1,2].

In this study we aimed to survey and critically evaluate the information concerning three diseases of hepatological interest: chronic hepatitis (CH), hemochromatosis (HH) and Caroli's disease (CA) very different both in term of epidemiological impact, diagnostic strategies and therapeutic approaches. In accordance with a validated method [3], the three search terms were entered into four English-language search engines (Altavista [www.altavista.com], Yahoo [www.yahoo.com], Lycos [www.lycos.com] and Google [www.google.com]), and the first five links leading to relevant content were considered (accounting for a total of 60 sites). The objective items, assessed by three operators, were: the type of medical information offered (official vs. alternative medicine), the major target (physicians vs. patients vs. both), the commercial sponsorship (present vs. absent; in the case of sponsored sites, the presence of financial disclosure was also considered), the frequency of updates (≤ 6 vs. > 6 months), the presence of site entry restriction (present vs. absent), the statement of authorship (i.e. a clear indication of the author's name and

qualifications: present vs. absent), the attribution of the source of content (i.e. references to scientific literature: present vs. absent). The characteristics of the web sites were described and their quality evaluated by three independent reviewers who assigned a score ranging from 1 to 5 for accuracy, reliability and depth. An overall quality score was calculated for each site on the basis of the mean of the scores awarded to the three quality items of accuracy, reliability

Table 1
Relationship between the characteristics of 60 hepatological websites and mean overall quality score as derived from univariate and multivariate logistic regression analysis. Odds ratios (OR) for insufficient score with 95% confidence intervals (in parentheses) are given for each site. Statistically significant results in bold

Variables	Statistical analysis	
	Univariate	Multivariate
Disease		
CH vs. HH	1.5 (0.4–5.2)	0.13 (0.2–6.8)
CH vs. CA	2.8 (0.8–10.0)	0.6 (0.1–3.5)
Type of the site		
Commercial vs. non-commercial	21.2 (2.5–177.3)	18.1 (1.7–192.5)
Update of the site		
> 6 vs. ≤ 6 months	1.9 (0.6–6.0)	2.7 (0.5–12.5)
Attribution of source of content of the site		
Absent vs. present	2.8 (0.9–8.5)	1.9 (0.4–7.7)

CH: chronic hepatitis; HH: hereditary hemochromatosis; CA: Caroli's disease

the diagnosis of genetic Δ^4 -3-oxosteroid 5 β -reductase deficiency and in presence of 3-oxo- Δ^4 bile aciduria it should help to distinguish a genetic defect from a secondary defect.

Acknowledgements

The authors thank Dr Kenneth D.R. Setchell and Nancy C. O'Connell (Cincinnati Children's Hospital, Ohio, USA) for performing fast atom bombardment ionization mass spectrometry analysis.

Emmanuel Gonzales^{1,3}, Danièle Cresteil³,
Christiane Baussan², Alain Dabadie⁵, Marie-
Françoise Gerhardt⁴, Emmanuel Jacquemin^{1,3}

¹Hepatology Unit, Department of Pediatrics,
Bicêtre University Hospital, 94275
Le Kremlin Bicêtre Cedex, France

²Biochemistry, Assistance Publique-Hôpitaux de Paris,
Bicêtre University Hospital, 94275
Le Kremlin Bicêtre Cedex, France

³INSERM U 347, Bicêtre University Hospital, 94275
Le Kremlin Bicêtre Cedex, France

⁴Biochemistry, St Joseph Hospital, 75674
Paris Cedex 14, France

⁵Pediatric Department, Rennes University Hospital, 35056

Rennes Cedex 2, France

E-mail address: emmanuel.jacquemin@bct.ap-hop-paris.fr

References

- [1] Setchell KDR, Suchy FJ, Welsh MB, Zimmer-Nechemias L, Heubi J, Balistreri WF. Δ^4 -3 oxosteroid 5 β -reductase deficiency described in identical twins with neonatal hepatitis. A new inborn error in bile acid synthesis. *J Clin Invest* 1988;82:2148–2157.
- [2] Clayton PT, Patel E, Lawson AM, Carruthers RA, Tanner MS, Strandvik B, et al. 3-oxo- Δ^4 bile acids in liver disease. *Lancet* 1988;1: 1283–1284.
- [3] Sumazaki R, Nakamura N, Shoda J, Kurosawa T, Tohma M. Gene analysis in Δ^4 -3 oxosteroid 5 β -reductase deficiency. *Lancet* 1997;349: 329.
- [4] Daugherty CC, Setchell KDR, Heubi JE, Balistreri WF. Resolution of liver biopsy alterations in three siblings with bile acid treatment of an inborn error of bile acid metabolism (Δ^4 -3-Oxosteroid 5 β -reductase deficiency). *Hepatology* 1993;18:1096–1101.
- [5] Charbonneau A, Luu-The V. Genomic organization of a human 5 β -reductase and its pseudogene and substrate selectivity of the expressed enzyme. *Biochim Biophys Acta* 2001;1517:228–235.
- [6] Lemonde HA, Custard EJ, Bouquet J, Duran M, Overmars H, Scambler PJ, et al. Mutations in SRD5B1 (AKR1D1), the gene encoding Delta(4)-3-oxosteroid 5beta-reductase, in hepatitis and liver failure in infancy. *Gut* 2003;52:1494–1499.

doi:10.1016/j.jhep.2003.12.024

Tumor necrosis factor-related apoptosis-inducing ligand (TRAIL) during liver regeneration

To the Editor:

We read with great interest the article "Hepatitis B virus enhances tumor necrosis factor-related apoptosis-inducing ligand (TRAIL) cytotoxicity by increasing TRAIL-R1/death receptor 4 expression" by Janssen et al. [1], particularly since a role for TRAIL in HBV hepatitis is not well elucidated. Another study also suggests that TRAIL plays an important role in eliminating virus-infected cells by inducing apoptosis via caspase-dependent pathway [2].

TRAIL is also known to induce nuclear factor- κ B (NF- κ B) activation as well as apoptosis in various cells, although the switching mechanism of these two different signalings is not well known. In mice model of liver regeneration, NF- κ B activation occurs rapidly within 30 min after hepatectomy [4]. Additionally, TNF α is up-regulated in serum and liver tissues in the early stage of liver regeneration [5], and Fas engagement accelerates liver regeneration after partial hepatectomy [6]. Collectively, these observations suggest that TRAIL expression may have a role in liver regeneration.

Therefore, we investigated serum TRAIL concentrations during liver regeneration in nine healthy donors before and

after undergoing surgery for liver tissue resection for donation. Seven of the nine donors were for right lobe grafts, and the remaining two donors were for lateral graft. The average rate of graft volume per total liver volume was 61.3% (right) and 21.8% (lateral). Blood samples of the nine healthy patients were obtained before surgery, at 6 h post-operative and then daily to post-operative day 10. The serum TRAIL levels were measured by ELISA (BioSource International, Inc., Camarillo, CA). Before surgery, mean serum TRAIL levels were 500 ± 122 pg/ml before the operation. A rapid decrease in serum TRAIL was observed after resection, reaching a nadir at 12 h post-hepatectomy, followed by a gradual increase after post-operative day 3 (POD3) (Fig. 1). There was no difference in TRAIL levels between graft types. These results suggested that TRAIL expression was down-regulated during liver regeneration, in contrast to up-regulation of other cytokines, such as TNF α , IL-1, IL-6 [5] or IL-18 (unpublished data) that can also activate NF- κ B.

Although TRAIL is tough to kill selectively tumor cells, TRAIL activity can also lead to massive apoptosis of primary human hepatocytes [3]. Natural killer (NK) cells

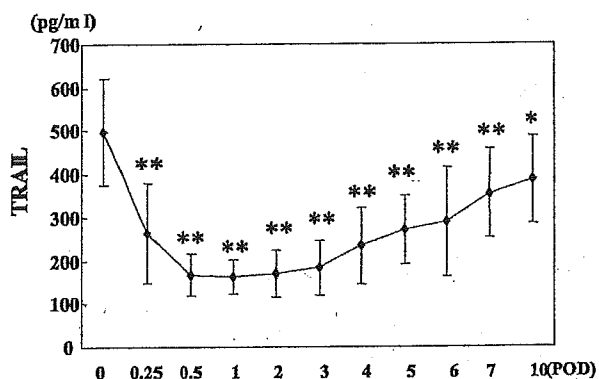


Fig. 1. Serum TRAIL concentrations before and after hepatectomy in donors. Bars indicate standard deviation (Paired Student's *t*-test; **p* < 0.05 and ****p* < 0.01).

strongly and constitutively express TRAIL and these cells participate in the host defense to viral infection and tumor metastasis, indicating that the physiological TRAIL levels are not cytotoxic toward normal hepatocytes. Our findings demonstrate that serum TRAIL levels decrease during liver regeneration, and indicating a negative modulatory role for TRAIL during hepatocyte proliferation. Thus, TRAIL expression may contribute to pathways that impair cell proliferation of hepatocytes after partial hepatectomy. Further evaluation of these possible roles for TRAIL activity and regulation of TRAIL expression during liver regeneration will provide insight into pathways that control hepatocyte cell proliferation and death.

Yumi Yamaguchi¹, Katsuya Shiraki¹, Yukiko Saito¹, Takeshi Nakano², Shugo Mizuno², Shinji Uemoto²

¹First Department of Internal Medicine,
Mie University School of Medicine,
2-174 Edobashi, Tsu,
Mie 514-8507, Japan

²First Department of Surgery,
Mie University School of Medicine,
2-174 Edobashi, Tsu,
Mie 514-8507, Japan

E-mail address: katsuyas@clin.medic.mie-u.ac.jp

References

- [1] Janssen HL, Higuchi H, Abdulkarim A, Gores GJ. Hepatitis B virus enhances tumor necrosis factor-related apoptosis-inducing ligand (TRAIL) cytotoxicity by increasing TRAIL-R1/death receptor 4 expression. *J Hepatol* 2003;39:414–420.
- [2] Mundt B, Kuhnel F, Zender L, Paul Y, Tillmann H, Trautwein C, et al. Involvement of TRAIL and its receptors in viral hepatitis. *FASEB J* 2003;17:94–96.
- [3] Armeanu S, Lauer UM, Smirnow I, Schenk M, Weiss TS, Gregor M, Bitzer M. Adenoviral gene transfer of tumor necrosis factor-related apoptosis-inducing ligand overcomes an impaired response of hepatoma cells but causes severe apoptosis in primary human hepatocytes. *Cancer Res* 2003;63:2369–2372.
- [4] Schmid RM, Adler G. NF-kappaB/rel/IkappaB: implications in gastrointestinal diseases. *Gastroenterology* 2000;118:1208–1228.
- [5] Slotwinski R, Olszewski WL, Paluszkiwicz R, Zieniewicz K, Hevelke P, Zaleska M, et al. Serum cytokine concentration after liver lobe harvesting for transplantation. *Ann Transplant* 2002;7:36–39.
- [6] Desbarats J, Newell MK. Fas engagement accelerates liver regeneration after partial hepatectomy. *Nat Med* 2000;6:920–923.

doi:10.1016/j.jhep.2003.12.016

Significance of CT Attenuation Value in Liver Grafts Following Right Lobe Living-Donor Liver Transplantation

Taku Iida^{a,*}, Shintaro Yagi^a, Kentaro Taniguchi^a, Tomohide Hori^a, Shinji Uemoto^a, Kouichiro Yamakado^b and Taizo Shiraishi^c

^aFirst Department of Surgery, ^bRadiology and ^cSecond Department of Pathology, Mie University, Tsu, Mie, Japan
*Corresponding author: Dr. Taku Iida, i-taku@clin.medic.mie-u.ac.jp

In adult living-donor liver transplantation (LDLT), the assessment of the allograft functional reserve is important for adequate graft regeneration. From March 2002 to December 2003, 30 adult recipients underwent right lobe LDLT. Mean CT attenuation values (CT-AVs) in the graft were measured on unenhanced CT for 6 months after LDLT. The histological features of the graft parenchyma were evaluated with post-operative liver biopsy specimens. Mean CT-AVs after LDLT were decreased significantly from the pre-operative values, recovered to over 60 HU within 6 months. There was a positive linear correlation between the CT-AVs and the receptor index (LHL15) in technetium-99m-diethylenetriaminepenta-acetic acid-galactosyl-human serum albumin (^{99m}Tc-GSA) liver scintigraphy ($r = 0.803$, $p = 0.005$). The recipients were divided into two groups according to the CT-AV at one post-operative week (group H; ≥ 55 HU, group L; < 55 HU). The low CT-AVs, under 55 HU, in group L were prolonged for 3 months compared with those in group H ($p < 0.05$). The 1-year cumulative survival rate was 94.7% and 45.5% in groups H and L, respectively ($p = 0.014$). Histological findings revealed that the parenchymal damage was severe in the grafts with low CT-AVs. The CT-AVs in the grafts may be a useful parameter for assessing the allograft functional reserve.

Key words: CT attenuation value, graft function, living-donor liver transplantation

Received 24 June 2004, revised 30 November 2004 and accepted for publication 6 December 2004

Introduction

Living-donor liver transplantation (LDLT) and split liver transplantation (SLT) have been accepted as treatment for

end-stage liver diseases worldwide, to overcome the shortage of organs from cadavers.

Liver regeneration of a segmental liver graft is essential in adult LDLT or SLT. However, recipients often suffer from prolonged cholestasis, coagulopathy and massive ascites due to impairment of liver regeneration with small-for-size grafts (1). In addition to the assessment of the graft volume, quantitative and qualitative evaluation of the liver allograft function reserve may be necessary for proper graft regeneration.

Hemodynamics changes dramatically after liver transplantation, which influences the sinusoidal and hepatic parenchymal conditions. Therefore, several complications are possible such as the sinusoidal destruction (2) and hepatocyte ballooning, congestion (3), necrosis, and fat infiltration (4) in the graft parenchyma, especially in small-for-size grafts.

We focused on the parenchymal morphological changes in the graft, and tried to evaluate quantitatively with the mean CT attenuation value (CT-AV). The aim of the present study was to evaluate the feasibility of assessing the allograft functional reserve.

Patients and Methods

Patients

The subjects were 30 adult patients who underwent LDLT using right-lobe graft between March 2002 and December 2003, comprised of 23 men and 7 women ranging from 20 to 67 years old (median, 53 years). Their body weight ranged from 39.6 to 89.4 kg (median, 60.1 kg).

The etiologies of their liver disease were hepatocellular carcinoma with liver cirrhosis in 15 patients, hepatitis B or C virus (HBV/HCV)-related cirrhosis in six, acute liver failure in three, primary biliary cirrhosis in three, primary sclerosing cholangitis in two and alcoholic cirrhosis in one.

Donors and grafts

The donors comprised 13 males and 17 females (1 parent; 12 spouses; 3 siblings; 12 children; 1 cousin and 1 grandson), ranging in age from 18 to 62 years old (median, 42.5 years). Twenty-nine grafts were ABO-compatible with the recipients, and one graft was ABO-incompatible. The graft-type comprised 28 right lobes, and 2 right lobes with the middle hepatic vein. The actual graft weight ranged from 460 to 1180 g (median, 660 g). The

Significance of CT Attenuation Value in Liver Grafts

graft-to-recipient weight ratio (GRWR) ranged from 0.83% to 1.53% (median, 1.09%).

After evaluation of the MHV tributaries draining the anterior segment by pre-operative dynamic CT, we selected the graft-type. To solve the problem of potential venous congestion in the anterior segment, we selected right lobe grafts with the MHV in MHV-dominant donors, if the remnant liver volume was more than 35% of the whole liver by CT volumetry. Whenever these conditions were not satisfied, right lobe grafts without the MHV were used. All the branches of the MHV (V5, V8) of a significant size (>7 mm) were preserved with a caval cuff and reconstructed in an end-to-side fashion to the anterior wall of the inferior vena using autologous venous grafts. Twenty-four of the 30 grafts had significant accessory hepatic veins, which were reconstructed.

Mild (<30%) macrovesicular steatosis was histologically confirmed in eight grafts, and there were no moderate or severe steatotic grafts.

Immunosuppression

The immunosuppression protocol consisted of tacrolimus and low-dose steroids. The target whole-blood trough level for tacrolimus was 10–12 ng/mL during the first 2 weeks, approximately 10 ng/mL thereafter, and 5–10 ng/mL from the second month. Steroid therapy was initiated at a dose of 10 mg/kg of methylprednisolone before reperfusion from the portal vein, then tapered from 1 mg/kg per day 1 to 0.3 mg/kg per day until the end of the first month. During the post-operative period, 1 mg/kg per day of the same drug was given for the first 3 days, followed by 0.5 mg/kg per day for the next 3 days. This was changed to oral prednisolone at a dose of 0.3 mg/kg per day 7 days after LDLT. Prednisolone was reduced to 0.1 mg/kg per day 1 month after LDLT, and patients were weaned off steroids at around 3–6 months post-operatively if their liver function was stable.

Measurement of CT-AV of the graft

Helical CT studies were conducted with a CT-high speed QXI (GE Medical Systems, Tokyo, Japan). The scanning parameters were 120 kV, 200 mA, collimation at 5 mm, and a table speed of 10 mm/s, with reconstruction increments of 5 mm.

For each case, measurement of the CT-AVs (expressed in Hounsfield units: HU) of the graft parenchyma were made with 10 randomly placed, circular regions of interest (ROI) with a cursor 3 mm in diameter, on both the anterior and posterior segments on five transverse sections at different hepatic levels on non-enhanced CT (5). To avoid the partial-volume averaging effects, obvious necroses or segmental congestion, vascular and biliary systems in the graft, areas of artifact, and areas near the edge of organs were excluded from these measurements. The mean CT-AV of the ROI was calculated from measurements at 1, 2, 3 and 4 weeks, and 3 and 6 months after LDLT. Pre-operative CT-AVs were the donor's pre-operative values.

All helical CT studies were performed under same configurations in all recipients and donors.

Technetium-99m-diethylenetriaminepenta-acetic acid-galactosyl-human serum albumin (^{99m}Tc-GSA) liver scintigraphy & the receptor index (LHL15)

Seven recipients (gross, 10 examinations) underwent technetium-99m-diethylenetriaminepenta-acetic acid-galactosyl-human serum albumin (^{99m}Tc-GSA) liver scintigraphy at 2 and 4 weeks after LDLT. ^{99m}Tc-GSA was supplied by Nihon Medi-Physics (Nishinomiya, Japan). After intravenous injection of 185Mq of ^{99m}Tc-GSA, dynamic imaging was performed with the patient supine using a large field-of-view gamma camera (GCA 7200A

gamma camera; Toshiba, Tokyo, Japan). ROIs were defined for the liver and heart using standard imaging software which was used to create time-activity data.

The receptor index (LHL15) is calculated by dividing the radioactivity of the liver ROI by the radioactivity of the whole liver (graft) plus heart ROIs 15 min after the injection, according Kudo et al. (6).

CT volumetry

CT volumetry for recipients was performed for measurement of the graft volume (GV) at 1, 2, 3 and 4 weeks, and 3 and 6 months after LDLT. The outline of the graft in each slice was traced with ROIs. The graft area was calculated using an image-processing program (Advantage Workstation: GE Medical Systems, Tokyo, Japan), and total GV was finally calculated by integrating images from each graft region. The recipient's standard liver volume (SLV) was determined according to the Urata equation (7), and the GV/SLV ratio was calculated.

Histological analysis

All of the histologic specimens were obtained from a needle biopsy of the right lobe grafts using a 16-gauge biopsy needle for the post-operative evaluation of liver dysfunction. Tissue specimens were fixed in 4% phosphate-buffered saline-buffered formalin, embedded in paraffin, sectioned and stained with hematoxylin-eosin by standard histological techniques. With the modified semi-quantitative scoring system for histological features of hepatic parenchyma (hepatocyte ballooning, hepatocyte necrosis, congestion, microvesicular fat, neutrophil aggregates, cholestasis) according to Neil et al. (8) (Table 1), an experienced liver pathologist reviewed the histological findings.

Protocol biopsy has not been performed in our institute.

Statistical analyses

Statistical analysis was performed using Mann-Whitney for discontinuous data, Student's t-test for continuous data, and the Cox-Mantel test for Kaplan-Mayer survival analysis. The correlations were analyzed by Pearson test. Values of $p < 0.05$ were considered significant. Values are presented as mean \pm SD.

Table 1: Semi-quantitative scoring system for histological features in the graft parenchyma

Ballooning	0. No 1. Yes
Hepatocyte necrosis	0. None 1. Small foci 2. Confluent areas 3. Bridging necrosis
Congestion	0. No 1. Yes
Microvesicular fat	0. None 1. <1/3 hepatocytes 2. Between 1/3 and 2/3 hepatocytes 3. >2/3 hepatocytes
Neutrophil aggregates	0. None 1. Minimal 2. Moderate 3. Extensive
Cholestasis	0. None 1. Mild 2. Moderate 3. Severe

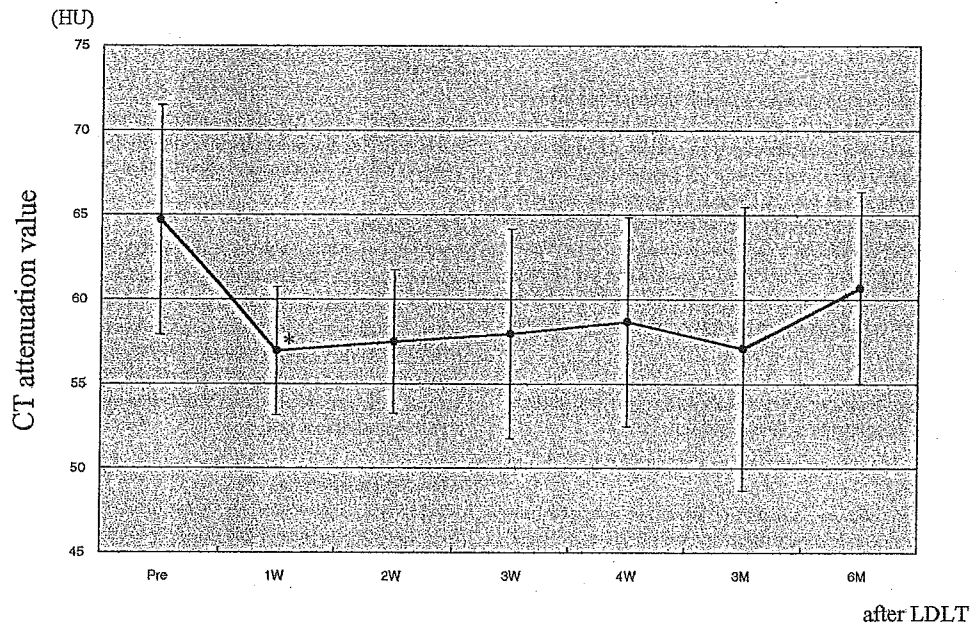


Figure 1: Changes in CT-AVs following LDLT. * $p < 0.05$ pre-operative CT-AV versus CT-AV at 1 week after LDLT. Pre-operative: $n = 30$, 1 week: $n = 30$, 2 weeks: $n = 27$, 3 weeks: $n = 26$, 4 weeks: $n = 27$, 3 months: $n = 20$, 6 months: $n = 15$, respectively.

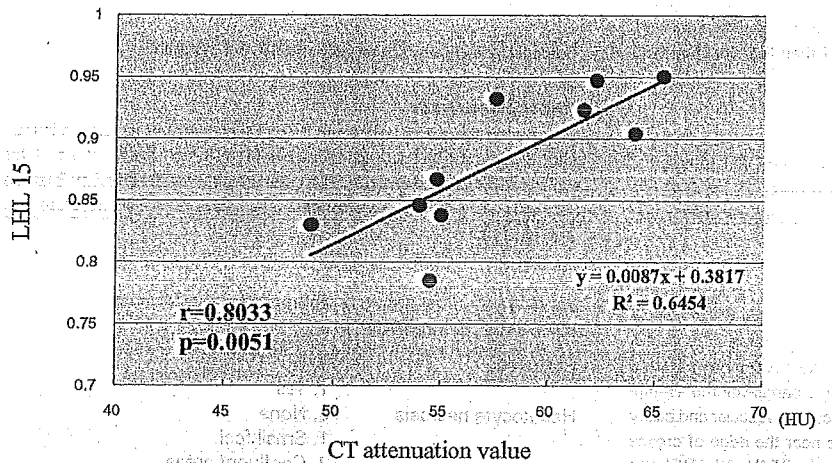


Figure 2: Correlation between CT-AV in the graft and LHL15. Seven recipients (gross, 10 examinations) underwent ^{99m}Tc -GSA liver scintigraphy at 2 and 4 weeks after LDLT. There was a significant positive linear correlation ($r = 0.803$, $p = 0.005$).

Results

Changes in CT-AVs following LDLT

The changes in mean CT-AVs (mean \pm SD of all grafts) are shown in Figure 1. The pre-operative mean CT-AV of 64.7 ± 6.8 HU decreased significantly to 56.9 ± 3.8 HU ($p < 0.05$) at 1 week after transplantation. Thereafter, the mean CT-AV remained under 60 HU for 3 months after LDLT. The mean CT-AV recovered to over 60 HU (60.7 ± 5.7 HU) at 6 months after LDLT.

Correlation between CT-AV and LHL15

Figure 2 shows the relationship between CT-AV and LHL15 in 10 examinations on the same day in 7 recipients. There was a significant positive linear correlation between the CT-AV and LHL15 ($r = 0.803$, $p = 0.005$).

Changes in CT-AVs in subgroups

The recipients were divided into two groups according to the CT-AV at 1 week after LDLT. Group H (high CT-AV) consisted of 19 recipients with a mean CT-AV of more than

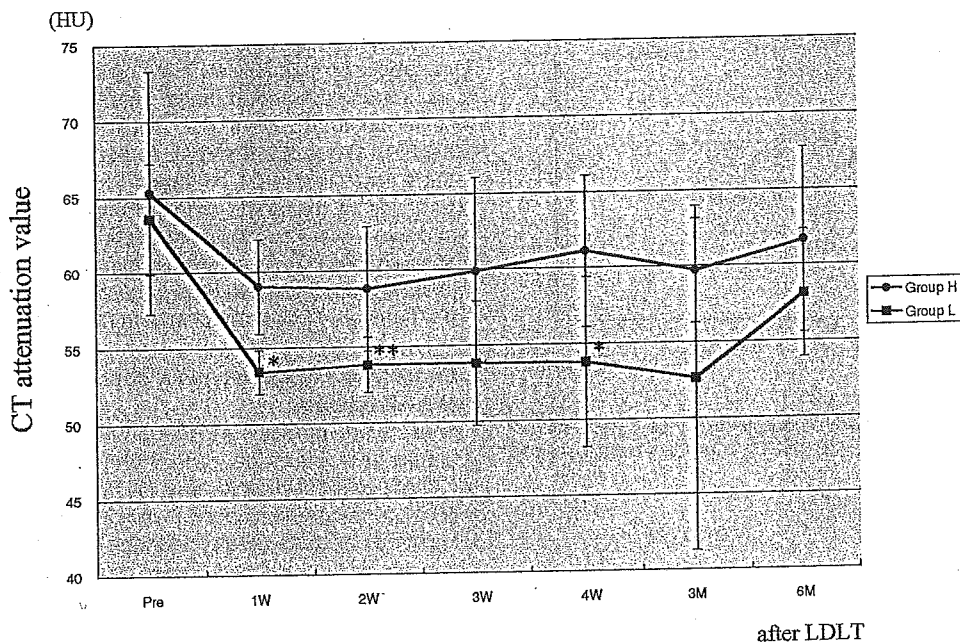


Figure 3: Changes in CT-AVs in subgroups. * $p < 0.05$ group H versus L, pre-operative: group H, $n = 19$; group L, $n = 11$, 1 week: H, $n = 19$; L, $n = 11$, 2 weeks: H, $n = 19$; L, $n = 8$, 3 weeks: H, $n = 17$; L, $n = 9$, 4 weeks: H, $n = 18$; L, $n = 9$, 3 months: H, $n = 14$; L, $n = 6$, 6 months: H, $n = 10$; L, $n = 5$, respectively.

55 HU, and group L (low CT-AV) of 11 recipients with a mean CT-AV of less than 55 HU, respectively.

The changes in mean CT-AV in the two groups are shown in Figure 3.

There were no significant differences in the CT-AVs of the donors (pre-operative CT-AVs) between groups H and L (H, 65.3 ± 8.0 HU, L, 63.6 ± 3.6 HU, $p = 0.55$).

CT-AVs in both groups decreased at 1 week after LDLT. The CT-AVs in group H were increased at 3 weeks after LDLT, but the CT-AVs in group L were significantly lower during the 4 weeks after LDLT than those in group H (1 week: H, 59.0 ± 3.1 HU; L, 53.4 ± 1.4 HU; 2 weeks: H, 58.2 ± 4.1 HU; L, 53.8 ± 1.8 HU; 3 weeks: H, 59.9 ± 6.2 HU; L, 53.8 ± 4.1 HU; 4 weeks: H, 61.1 ± 4.9 HU; L, 53.8 ± 5.6 HU; $p < 0.05$).

The low CT-AVs in group L (3 months: 52.6 ± 11.3 HU) continued to decrease for 3 months after LDLT.

The CT-AVs recovered to about 60 HU in the two groups at 6 months (H, 61.6 ± 6.1 HU; L, 58.1 ± 4.2 HU).

On the other hand, there were significant differences between the pre-operative CT-AVs of the 32 non-steatotic grafts and 8 steatotic grafts (non-steatotic grafts, 68.0 ± 4.9 HU, steatotic grafts, 58.5 ± 5.3 HU, $p < 0.05$). In con-

trast, the changes in the post-operative CT-AVs in the mild steatotic grafts did not differ from those in non-steatotic grafts during 6 months after LDLT (data not shown).

The post-operative course of serum total bilirubin level

Serum total bilirubin levels in group L were significant higher than those in group H from 1 to 4 weeks after LDLT. Serum total bilirubin levels in group H were normalized within 6 months after LDLT, however, hyperbilirubinemia was prolonged until 3 months after LDLT in group L.

The post-operative course of coagulation profile

The post-operative prothrombin time international normalized ratio (PT-INR) levels in group H were restored to an almost normal level within 2 weeks after LDLT. In contrast, PT-INR levels in group L were significantly higher than those in group H for 3 months after LDLT.

Changes in size of the grafts

The GV/SVL ratio increased rapidly, to over 100%, 1 week after LDLT in all groups. The GV/SVL ratio in group L tended to be higher than that in group H for the 6 months after LDLT; in particular the GV/SVL ratio in group L was significantly higher at 4 weeks and 3 months than that in group H (4 weeks: H, 107%; L, 130%; 3 months: H, 104%; L, 133%, $p < 0.05$).

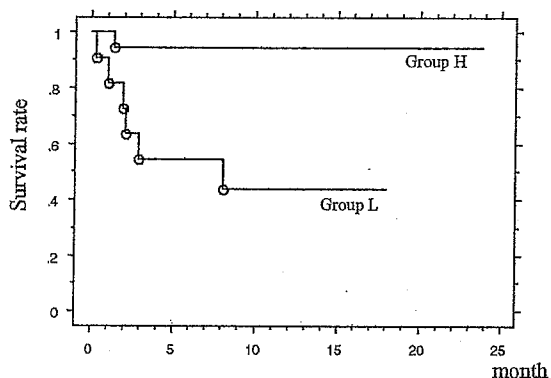


Figure 4: Actuarial survival in subgroups. The 1-year cumulative survival rate was 94.7% and 45.5% in groups H and L, respectively ($p = 0.014$).

Patient survival

Patient survival curves are shown in Figure 4. The 1-year cumulative survival rate was 94.7% and 45.5% in groups H and L, respectively ($p = 0.014$).

The causes of death were intra-cranial bleeding ($n = 1$) in group H, and graft failure ($n = 4$), pneumonia ($n = 1$) and cardiac failure ($n = 1$) in group L.

Regarding the four recipients in group L who died of graft failure, one died due to an immunological response related to ABO incompatibility at 54-days after LDLT. The other three recipients with high model end-stage liver disease (MELD) scores had emergency LDLT, and showed hyperbilirubinemia and coagulopathy that persisted post-

operatively without size mismatch. The liver grafts did not become sufficiently functional for the post-operative metabolic demands, which eventually led to graft failure, accompanied by deep fungal infection. The patients died at 56, 65 and 72 days after LDLT. The remaining five patients in group L are still alive. Furthermore, there were three cases in group L of stenosis of hepatic venous anastomoses of the grafts at 9, 13 and 18 days after LDLT, and these were successfully treated with stent insertions to the hepatic veins. However, hyperbilirubinemia, coagulopathy and massive ascites persisted for 2–3 weeks, and the recovery of liver function was delayed.

Comparison of the recipient data between the two groups

There were no significant differences between the two groups in recipient age, gender, graft-recipient weight ratio (GRWR), cold ischemic time (CIT), warm ischemic time (WIT), intra-operative blood loss or steatotic liver graft and incidence of acute cellular rejection or mean portal venous pressure during the first 3 days after LDLT. However, the MELD score, mean ascitic fluid volume during the 7 days after LDLT were significantly higher in group L than in group H (Table 2).

Histological findings

A gross of 41 post-operative liver biopsy specimens in 20 recipients were collected to diagnose the causes of liver dysfunction. Protocol biopsies are not performed in our institute. Therefore, liver biopsies were not performed on the nine recipients in group H who had no post-operative liver dysfunction during 6 months after LDLT, or the patient in group L who died at nine days after LDLT. Hence, liver biopsy specimens were obtained from a total of 10 recipients in group H and 10 recipients in group L.

Table 2: Comparison of the recipient data between the two groups

	Group H (n = 19)	Group L (n = 11)	p
Age	51.9 ± 12.6	51.3 ± 4.1	NS
Gender	M 16, F 3	M 7, F 4	NS
Etiology of liver disease	HCC 11, PBC 3, LC(B) 1, LC(C) 1; LC(alcohol) 1; ALF 1, PSC 1	HCC 4; LC(C) 4, LC(C) 1; LC(alcohol) 1; ALF 2; PSC 1	NS
MELD score	9.9 ± 7.3	18.2 ± 12.9	0.039
Graft-to-recipient weight ratio (%)	1.07 ± 0.23	1.05 ± 0.16	NS
Cold ischemic time (min)	105.4 ± 44.5	133.5 ± 81.2	NS
Warm ischemic time (min)	45.5 ± 18.4	47.2 ± 14.6	NS
Blood loss (mL)	20249 ± 18613	18287 ± 16149	NS
Steatotic graft (mild macrovesicular steatosis)	6 cases	2 cases	NS
Incidence of acute cellular rejection	26.3% (5/19)	27.3% (3/11)	NS
Mean portal venous pressure (mmHg) [†]	24.8 ± 7.4	26.0 ± 6.8	NS
Mean ascitic fluid volume (mL) [‡]	1111.4 ± 952.8	2216.6 ± 1380.5	.02

M: Male; F: Female; MELD: Model for end-stage liver disease; HCC: Hepatocellular carcinoma; PBC: Primary biliary cirrhosis; PSC: Primary sclerosing cholangitis; LC: Liver cirrhosis; ALF: Acute liver failure.

[†]During first 3 days after LDLT.

[‡]During 7 days after LDLT.

Significance of CT Attenuation Value in Liver Grafts

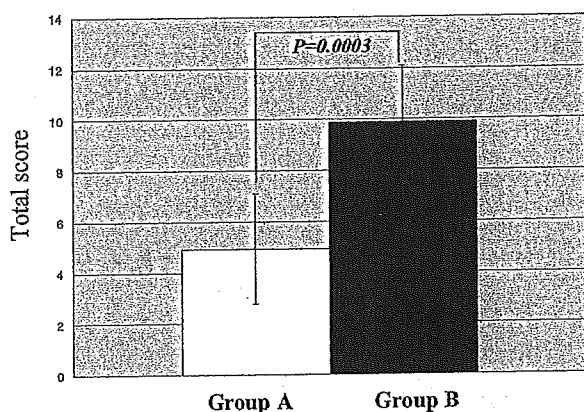


Figure 5: Total scores of parenchymal features in the two groups. Total scores, representing liver damage, were calculated to sum up the scores of parenchymal features. The total score in group A was 4.94 ± 2.15 , and in group B was 9.88 ± 2.20 ($p = 0.0003$).

The specimens were divided into two groups: group A ($n = 23$), in which the biopsy was performed on grafts with $CT-AV \geq 55$ HU, and group B ($n = 18$), in which the biopsy was performed on grafts with $CT-AV < 55$ HU.

There were significant differences between the two groups for the scores of hepatocyte necrosis ($p < 0.0001$), congestion ($p = 0.0093$) and microvesicular fat ($p = 0.0002$).

On the other hand, the scores for hepatocyte ballooning, neutrophil aggregates and cholestasis did not differ significantly between the two groups.

The total scores in group A were significantly lower than those in group B (A: 4.94 ± 2.15 vs. B: 9.88 ± 2.20 , $p = 0.0003$) (Figure 5).

Among all specimens, there was a significant negative linear correlation between the $CT-AV$ and total score ($r = -0.841$, $p < 0.0001$) (Figure 6). The histological evaluations of the biopsy specimens revealed that the parenchymal damage was severe in the group with low $CT-AV$, compared to that in the group with high $CT-AV$.

Discussion

Adequate allograft regeneration is important in adult partial liver transplantation. Graft dysfunction, characterized by enhanced cholestasis, coagulopathy, and massive ascites, may occur in small-for-size grafts (1). Therefore, post-operative assessment of allograft function reserve is important for regeneration after LT, in addition to simple measurement of the graft volume. Namely, increased graft

volume without functional reserve implies only the hypertrophy of the graft, not true liver regeneration. Regardless of the suitability of the liver function, the GV/SLV ratio was increased in the present study. Consequently, the GV/SLV ratio is ineligible as an indicator of liver regeneration.

$CT-AV$ is expressed as an absolute value called the Hounsfield number in unenhanced CT. It has been well recognized since the late 1970s that unenhanced CT is useful for the detection of hepatic macrovesicular steatosis with a difference between liver and spleen $CT-AV$ (9). In LDLT, $CT-AV$ is used as a pre-operative evaluation of hepatic steatosis for donor selection (5,10).

Generally, low $CT-AVs$ in the liver imply the presences of steatosis, necrosis or congestion (11). Several reports have referred to morphological changes in the graft after LT such as destruction of sinusoidal lining cells, hepatocyte ballooning (2), congestion and hemorrhagic infiltration (3), necrosis and microvesicular steatosis (4). So, we tried to evaluate these morphological changes after LDLT quantitatively using $CT-AVs$.

With regard to the assessment of hepatic functional reserve, the indocyanine green (ICG) clearance test is a widely accepted procedure in liver surgery. However, this test is known to accurately reflect the effective hepatic blood flow, linked to the hepatocyte volume, and infra- and extrahepatic shunts. Therefore, discrepancies between ICG R15 and histological findings of the liver are seen. Furthermore, the ICG test is not reliable for accessing the hepatic function in patients with severe jaundice.

On other hand, $^{99m}Tc-GSA$, which binds specifically to asialoglyco-protein receptors on the hepatocellular membrane, is apparently useful for assessing hepatic function in patients with liver dysfunction under various physiological and pathological conditions, providing an important quantitative parameter of hepatic function that is totally independent of the ICG test.

Because $^{99m}Tc-GSA$ scintigraphy can determine the functioning hepatocyte mass, this procedure is acceptable for the evaluation of remnant liver function in liver surgery (12).

Recently, the liver allograft functional reserve in liver transplant recipients has been evaluated by $^{99m}Tc-GSA$ (13); and

The receptor index LHL15 is a simple indicator calculated from three-point data in time-activity curves, and significant correlations between LHL15 and conventional liver function tests have been reported (6,14).

Although $^{99m}Tc-GSA$ scintigraphy is a very sophisticated test for hepatic function, this examination is clinically more complicated for recipients in a serious condition, especially those in intensive care after LDLT, than unenhanced CT .